

## Surface-passivation-induced optical changes in Ge quantum dots

F. A. Reboredo\* and Alex Zunger

National Renewable Energy Laboratory, Golden, Colorado 80401

(Received 25 September 2000; published 29 May 2001)

One of the most interesting properties of quantum dots is the possibility to tune the band gap as a function of their size. Here we explore the possibility of changing the lifetime of the lowest-energy excited state by altering the surface passivation. We show that a moderately electronegative passivation potential can induce long-lived excitons without appreciable changes to the band gap. In addition, for such passivation the symmetry of the valence-band maximum is  $\gamma_{8v}$  ( $t_1$  derived) instead of the more usual  $\gamma_{8v}$  ( $t_2$  derived). This reverses the effect of the exchange interaction on the bright-dark exciton splitting.

DOI: 10.1103/PhysRevB.63.235314

PACS number(s): 78.67.Hc, 73.21.La, 71.35.-y

### I. INTRODUCTION

The order of the single-particle energy levels of different symmetries in nanostructures controls much of their optical and transport properties. In near-spherical quantum dots made of either diamond-like (Si, Ge) or zinc-blende (InP, InAs) materials, the allowed single-particle orbital symmetries are  $a_1$ ,  $a_2$ ,  $e$ ,  $t_1$ , and  $t_2$ . These orbital symmetries give rise to specific selection rules. These global symmetries can be rationalized, in the context of the envelope-function approximation, as the product of the symmetry of the underlying bulk Bloch function (e.g.,  $\Gamma_{15v}$  and  $\Gamma_{1c}$ , that transform as  $t_2$  and  $a_1$ , respectively) and the envelope function (e.g.,  $a_1$  and  $t_2$ , that are most  $s$  and  $p$  like respectively). As shown in Table I, one can distinguish a few cases of orbital symmetries and the resulting excitonic symmetries. For example, the most commonly encountered cases (labeled ‘‘case I’’) of direct-gap nanostructures (InP, GaAs, CdS) involves a valence band of  $t_2$  symmetry (made of a  $\Gamma_{15v}$  Bloch state and an  $a_1$  envelope) and a conduction band of  $a_1$  symmetry (made of an  $\Gamma_{1c}$  Bloch state and an  $a_1$  envelope). The direct product  $t_2 \times a_1$  of the electron and hole symmetries gives the orbital symmetry of the excitonic wave function. In this case the 12-fold degenerate-dipole-allowed  $T_2$ . Consideration of electron-hole exchange<sup>1,2</sup> splits  $T_2$  into singlet  $^1T_2$  and triplet  $^3T_2$ , being, respectively, spin allowed and spin forbidden. In the presence of spin orbit (see below) the ground state  $^3T_2$  is split into a lower fivefold-degenerate *forbidden*  $E+T_1$  multiplet and a higher allowed  $T_2$ . Case II involves a valence band of  $t_1$  symmetry (made again of a  $\Gamma_{15v}$  Bloch function but with a  $t_2$  envelope). If we consider the same  $a_1$ -symmetric conduction band as before, the exciton resulting of the direct product  $t_1 \times a_1 = T_1$  is now spatially forbidden for dipole transitions: Exchange splits it into a singlet  $^1T_1$  and a triplet  $^3T_1$ . In the presence of spin orbit the ground state is fivefold degenerate,  $E+T_2$ , which includes the *dipole-allowed* component  $T_2$ . We see that the question whether the valence-band maximum (VBM) has  $t_2$  or  $t_1$  orbital symmetry (or in other words, if the VBM envelope has a node or not) can decide if the exciton at threshold is orbital allowed, i.e., has a short radiative lifetime or not.

In the past it was noted that, assuming an infinite potential barrier around the dot, the order of  $t_1$  and  $t_2$  valence-band

levels depends on the material and dot size. Using the  $\mathbf{k}\cdot\mathbf{p}$  method, Efros and co-workers<sup>3,4</sup> found a  $t_1$ -like valence band maximum (i.e., a  $p$ -like envelope) for small<sup>5</sup> dots made of low-spin-orbit material (light elements), whereas Delley and Steigmeier,<sup>6</sup> Ren,<sup>7</sup> and the present authors<sup>8</sup> found, neglecting spin orbit, that Si exhibits a transition between  $t_2$  and  $t_1$  VBM’s as the size of the dot is reduced.

The infinite barrier boundary conditions used in some simplified model calculations might not have captured the physical circumstances appropriate to real dots. Indeed, dots are often fabricated with a coating of a second material surrounding them, intended to passivate surface dangling bonds, provide confinement, and assist in (e.g., colloidal) growth process. Such surface passivants are not easily modeled as an infinite potential barrier, but are more realistically thought of as an electronic material in its own right, having some characteristic energy level(s). For example, one can use the highest occupied orbital of the passivant with energy  $E_p$  (measured with respect to vacuum) as its characteristic energetic marker. This  $E_p$  can have different ‘‘band alignments’’ with respect to the VBM of the dot: for electropositive passivants  $E_p$  will be above the dot’s VBM, whereas for electronegative passivants  $E_p$  could be well below the VBM.

Using spin-orbit-pseudopotential calculations for spherical surface-passivated Ge quantum dots, we show for intermediate size Ge dots (diameter  $D=37.2$  Å) that, as the passivants  $E_p$  move from the electropositive to electronegative regime, (i) the dot VBM symmetry changes from  $\gamma_{8v}(t_2)$  to  $\gamma_{8v}(t_1)$ , thus converting the lower exciton from being primarily spatially allowed  $T_2$  to spatially forbidden  $T_1$ ; and (ii) the Bloch content of the conduction-band minimum (CBM) changes from being  $X$  like to  $L$  like (iii) a strongly electronegative passivant shifts both transitions (i) and (ii) to smaller dot sizes. Moreover, while the above noted changes in symmetry can profoundly affect the radiative luminescence lifetime (longer for forbidden than for allowed excitons) and the ratio  $\Delta E_{VBM}/\Delta E_{CBM}$  between conduction and valence confinement energies,<sup>9</sup> the effect on the excitonic transition energy itself is surprisingly small, being tenths of a meV.

### II. METHOD OF CALCULATION

We consider approximately spherical Ge crystallites with  $T_d$  symmetry, centered around a Ge atom. The surface dan-

TABLE I. The single-particle symmetries of the VBM and CBM and the ensuing symmetry of the electron-hole exciton without ( $\Delta_x=0$ ) and with ( $\Delta_x\neq 0$ ) exchange interaction. We show how the single-particle symmetry evolves from that of the Bloch function ( $\Gamma_{15v}$  or  $\Gamma_{1c}$ ) times the envelope function ( $a_1$  or  $t_2$ ). Spin orbit is neglected here.

Case	VBM symmetry ( $\Delta_{so}=0$ )	CBM symmetry ( $\Delta_{so}=0$ )	Exciton ( $\Delta_x=0$ )	Exciton ( $\Delta_x\neq 0$ )	Example
I	$\mathbf{t}_2=\Gamma_{15v}\times a_1(s)$	$\mathbf{a}_1=\Gamma_{1c}\times a_1(s)$	$T_2(\times 12)$	${}^3T_2(\times 9)+{}^1T_2(\times 3)$	InP,CdSe
II	$\mathbf{t}_1=\Gamma_{15v}\times t_2(p)$	$\mathbf{a}_1=L_{1c}\times a_1(s)$	$T_1(\times 12)$	${}^3T_1(\times 9)+{}^1T_1(\times 3)$	Ge
III	$\mathbf{t}_2=\Gamma_{15v}\times a_1(s)$	$\mathbf{t}_2=\Sigma(L_{1c}+X_{1c})$	$A_1+E+T_2+T_1$	${}^{3,1}A_1+{}^{3,1}E+{}^{3,1}T_2+{}^{3,1}T_1$	Si,Ge

gling bonds are passivated with pseudoatomic potentials located at 1.06 Å from the Ge site, and possessing a single bound state at energy  $E_p$  which will be varied. We consider dots with radii ranging from 10.5 to 24.5 Å, containing 281–3049 Ge atoms, respectively. Single-particle energy levels and wave functions are obtained from the Hamiltonian<sup>10,11</sup>

$$H = -\frac{\hbar^2}{2\alpha m}\nabla^2 + \sum_{\mathbf{R}_{Ge}} v_{Ge}(\mathbf{r}-\mathbf{R}_{Ge}) + \sum_{\mathbf{R}_p} v_p^{(\eta)}(\mathbf{r}-\mathbf{R}_p). \quad (1)$$

Here  $m$  is the bare electron mass,  $\alpha$  is a small adjustment on the electron mass intended to improve the fit, and  $v_{Ge}$  and  $v_p^{(\eta)}$  are the atomic local empirical pseudopotentials<sup>11</sup> of Ge and the passivant atom, respectively. We represent the Ge pseudopotential in reciprocal space, using the functional form

$$v_{Ge} = a_1(q^2 - a_2)/(a_3 e^{a_4 q^2} - 1) + \beta v_{Ge}^{SO}, \quad (2)$$

where  $q$  is the reciprocal-lattice wave vector,  $\beta$  is a coefficient adjusted to obtain the spin-orbit splittings, and  $v_{Ge}^{SO}$  is the spin-orbit interaction matrix.<sup>12</sup> The coefficients of Eq. (2) were fitted at a plane-wave cutoff of 5 Ry to obtain the bulk band structure at high symmetry points, the effective masses at the band extrema, and the spin-orbit splittings. The fitting procedure gives  $\alpha = 1.190\,264\,5$  [Eq. (1)] and  $a_1 = 0.584\,954$ ,  $a_2 = 2.344\,131$ ,  $a_3 = 3.244\,96$ ,  $a_4 = 0.649\,70$ , and  $\beta = 0.213\,137$  in atomic units.

The passivation pseudopotential  $v_p^{(\eta)}$  is designed to remove all states from the gap due to dangling bonds (within 1.5 eV of the band edges), and at the same time to model the behavior of the dot with different generic chemical passivations via different  $E_p$  values. We use

$$v_p^{(\eta)}(q) = \frac{(1+\eta)}{2} \sum_{i=1}^3 b_i e^{-c_i q^2} + \frac{(1-\eta)}{2} b_4 e^{-c_4 q^2},$$

with  $b_1 = -0.1770$ ,  $c_1 = 0.1534$ ,  $b_2 = 0.029\,82$ ,  $c_2 = 0.085\,228$ ,  $b_3 = -0.010\,24$ ,  $c_3 = 0.630\,689$ ,  $b_4 = -0.1035$ , and  $c_4 = 0.3409$  in atomic units.<sup>13</sup> Here  $\eta$  is scanned to alter the passivation. For  $\eta = -1$  we find that the passivant has a single bound state<sup>14</sup> with  $E_p = -18$  eV  $= E_V - 12.9$  eV, while for  $\eta = 1$  we have  $E_p = -1.5$  eV  $= E_V + 3.6$  eV where  $E_V$  is the VBM of bulk Ge. In all cases

the gap is free of surface states and the wave function of the passivant bound state decays within  $\sim 0.5$  Å.

Total spin-orbit symmetries are obtained with the double group character table<sup>15</sup> for  $T_d$  rotating the spin coordinates.<sup>16</sup> Orbital symmetry contributions are obtained, omitting the spin rotation.<sup>8</sup> The excitons are calculated within the configuration interaction method.<sup>8,17</sup>

### III. CHANGE OF VBM FROM $T_2$ TO $T_1$

Figure 1 shows contour plots of the band-edge wave functions of a dot of 37.2 Å and 1207 Ge atoms, passivated with two types of passivants. In order to obtain graphical information about the symmetric structure of  $\psi(\mathbf{r})$  we plot  $|\psi(\mathbf{r})| \text{sgn}[\text{Re}(\psi_i(\mathbf{r}))]$ , where  $|\psi(\mathbf{r})| = \sqrt{\psi_{\uparrow}^*(\mathbf{r})\psi_{\uparrow}(\mathbf{r}) + \psi_{\downarrow}^*(\mathbf{r})\psi_{\downarrow}(\mathbf{r})}$  and  $\psi_{\uparrow}^*(\mathbf{r})$  and  $\psi_{\downarrow}(\mathbf{r})$  are the spin-up and spin-down components of the total wave function  $\psi(\mathbf{r})$ . We find that whereas the overall symmetry of the VBM remains  $\gamma_8$ , its envelope-function content changes with passivation. Because we include spin-orbit, the orbital symmetries are partially mixed.<sup>18</sup> For electropositive passivation [ $E_p = E_V + 0.8$  eV, Fig. 1(a)] the  $\gamma_8$  VBM is 98%  $t_2$ , whereas the  $\gamma_8(t_1)$  is 41 meV lower. For electronegative passivation [ $E_p = E_V - 12.9$  eV, Fig. 1(b)] the  $\gamma_8$  VBM is 97%  $t_1$ , whereas the  $\gamma_{8v}(t_2)$  state is 34 meV lower. The crossing between  $\gamma_8(t_1)$  and  $\gamma_{8v}(t_2)$  for a  $D = 37.2$  Å dot occurs for passivation potential  $E_p \approx E_V - 1.4$  eV. This crossing can be understood by studying the first-order energy shift of the state  $\psi_n$ , due to the surface passivation potential in Eq. (1):

$$\Delta\epsilon(n, \eta) = \langle \psi_n | \sum_{\mathbf{R}_p} v_p^{(\eta)}(\mathbf{r}-\mathbf{R}_p) | \psi_n \rangle. \quad (3)$$

It can be shown that  $\Delta\epsilon(n, \eta)$  scales as

$$\Delta\epsilon(n, \eta) \sim \alpha(n, E_p(\eta)) \frac{F[E_p(\eta)]}{R}, \quad (4)$$

where  $F[E_p(\eta)]$  is a negative term representing the interaction of the rapidly varying ‘‘Bloch part’’ of the wave function with the passivation potential  $v_p^{(\eta)}$ , the factor  $R^{-1}$  takes into account the size scaling of the amplitude of the square-envelope function of  $\psi_n$  as the size of the dot increases, and  $\alpha[n, E_p(\eta)]$  accounts for the extension of the envelope function into the positions of the passivants. Because  $\Delta\epsilon(n, \eta)$  is an integral over the passivation potential, it becomes increasingly negative as  $E_p \rightarrow -\infty$ . Although the bulk Ge pseudo-

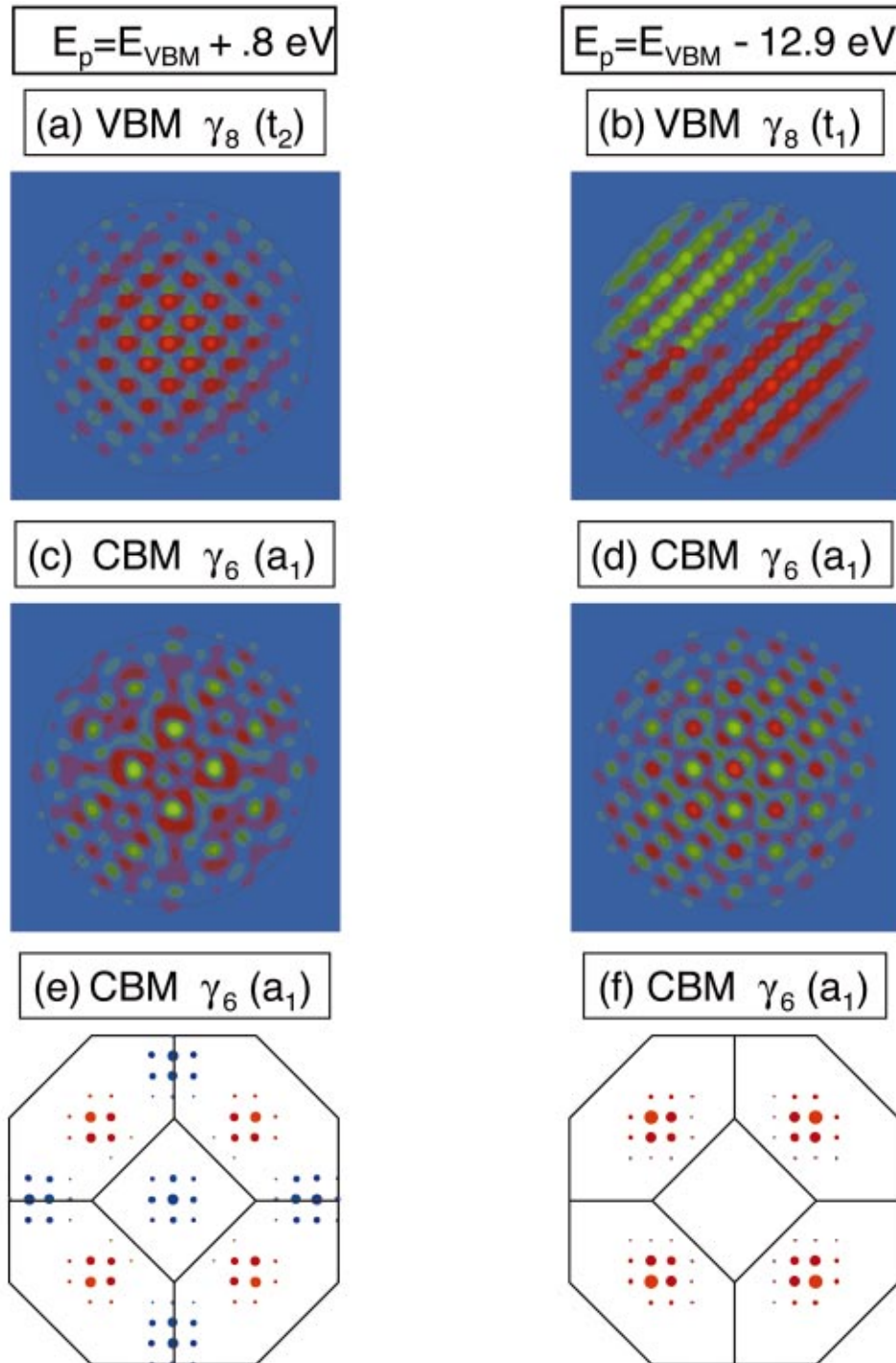


FIG. 1. (Color) (a)–(d) calculated wave functions of  $D=37.2 \text{ \AA}$  Ge dot, depicted along the (001) plane as explained in the text. Red indicates positive values, green corresponds to negative values, and light blue corresponds to zero values. (e) and (f) Bloch-function content of the CBM. Red points are close to the  $L$  minima, and blue points are close to the  $X$  minima.

potential and the size of the dot are fixed, a crossing between  $\gamma_{8v}(t_2)$  and the  $\gamma_{8v}(t_1)$  states can occur if  $\Delta\epsilon[\gamma_{8v}(t_2), \eta]$  is different from  $\Delta\epsilon[\gamma_{8v}(t_1), \eta]$  as a function of  $\eta$ . As can be seen in Fig. 1(a) the  $\gamma_{8v}(t_2)$  state has an  $a_1(s)$  envelope function for  $E_p = E_V + 0.8 \text{ eV}$ , while for  $E_p = E_V - 12.9 \text{ eV}$  [Fig. 1(b)] the  $\gamma_{8v}(t_1)$  VBM has a  $t_2(p)$  envelope. Because the  $s$ -like envelope function has the lowest angular momentum, within the single-band effective-mass approximation (EMA) treatment, and assuming infinite barriers, one would always obtain an  $s$ -like envelope for the VBM. Therefore, a  $p$ -like envelope might be seen as surprising. However, the

real structure of the wave function is more complex: the Bloch part of the VBM is a strongly varying spatial function, changing sign on an atomic scale [see Figs. 1(a) and 1(b)]. A node in the envelope function actually means that one of the nodes of the Bloch part is removed, which results in a lower kinetic energy. Therefore, for infinite barriers, the  $\gamma_{8v}(t_1)$  states [with a  $p$  envelope and a missing node] have a lower absolute energy than the  $\gamma_{8v}(t_2)$  state (with an  $s$  envelope). Because the  $s$ -like  $\gamma_{8v}(t_2)$  states indeed have one more node than  $p$ -like  $\gamma_{8v}(t_1)$  states, the  $\gamma_{8v}(t_2)$  have higher *total* angular momentum components than  $\gamma_{8v}(t_1)$ . Thus  $\gamma_{8v}(t_2)$

states can travel longer distances into the vacuum barrier, and have a larger amplitude at the passivant positions than  $\gamma_{8v}(t_1)$  states. This implies in Eq. (4) that  $\alpha[\gamma_{8v}(t_2)] > \alpha[\gamma_{8v}(t_1)]$ . Assuming that  $F[E_p(\eta)]$  is the same for  $\gamma_{8v}(t_2)$  and  $\gamma_{8v}(t_1)$ , a crossing between  $\gamma_{8v}(t_1)$  and  $\gamma_{8v}(t_2)$  states will occur when the difference in potential energy gained at the surface,  $(\alpha[\gamma_{8v}(t_2)] - \alpha[\gamma_{8v}(t_1)]) F[E_p(\eta)]/R$ , compensates for the kinetic energy saved by eliminating a node in the total wave function. Indeed, a direct calculation of Eq. (3) for the case of Fig. 1(b) shows that  $\Delta\epsilon[\gamma_{8v}(t_2), -1] - \Delta\epsilon[\gamma_{8v}(t_1), -1] = -72$  meV. Since the splitting between  $\gamma_{8v}(t_2)$  and  $\gamma_{8v}(t_1)$  is  $-34$  meV, the ‘‘kinetic part’’ of this splitting is 38 meV.

Equation (4) suggests that the passivation-induced splitting scales as  $AR^{-1}$ , where the coefficient  $A$  is increasingly negative as  $E_p \rightarrow -\infty$ . The critical size at which a  $\gamma_{8v}(t_2)$  to  $\gamma_{8v}(t_1)$  crossing occurs will depend on (i) the size scaling of the ‘‘kinetic part’’ splitting, and (ii) the passivation-induced splitting (which in turn depends  $E_p$ ). Our calculations suggest that the ‘‘kinetic part’’ of the splitting scales as  $BR^{-\gamma}$ , where  $B$  is positive and  $\gamma > 1$ . This implies that for intermediate passivation potentials ( $E_p \approx E_V - 1.4$  eV) larger dots would have a  $\gamma_{8v}(t_1)$  VBM and smaller dots a  $\gamma_{8v}(t_2)$  VBM. Indeed for  $E_p \approx E_V - 1.4$  eV, we find that for dots with diameters 28 and 37.2 Å,  $\gamma_{8v}(t_2)$  is above  $\gamma_{8v}(t_1)$  by 51 and 4 meV, whereas the level order is reversed for  $D = 50.9$  Å. For extremely electronegative potentials ( $E_p \approx E_V - 12.9$  eV), the VBM is always  $\gamma_{8v}(t_1)$ .

The passivation-induced  $t_1$ - $t_2$  crossing reported here behaves in an opposite way to the one predicted by Grigoryan *et al.*<sup>3</sup> within the  $\mathbf{k} \cdot \mathbf{p}$  method or infinite barriers and small spin-orbit couplings. In that case<sup>3</sup> the  $t_2$ -to- $t_1$  crossing was claimed to be due to a change of sign on the kinetic-energy splitting. In contrast here, we find that for Ge dots the kinetic energy part of the splitting is always positive. We believe that the kinetic part is positive as a result of the large (0.3 eV) spin-orbit splitting in Ge dots (which, according to Grigoryan *et al.*<sup>3</sup> favors  $t_2$ ) and the failure of the  $\mathbf{k} \cdot \mathbf{p}$  treatment on the very small size regime.

A study of the effect of passivation for Si dots was performed in the framework of the empirical tight-binding method by Xia and Cheah.<sup>19</sup> In this case an additional orbital, simulating the passivation, is added to the surface. Though this state can be thought of as analogous to our passivation potential, it is different in an important way. In the empirical tight-binding approach of Xia and Cheah, the Hilbert space at the surface is restricted to a state with energy  $E_p$ , thus excluding scattering-nonbonded states. Therefore, when  $E_p$  is sufficiently far from the band-edge energies, the second-order correction to the band-edge energies vanishes. However, in our calculation with passivation potentials, we do not truncate the Hilbert space at the band-edge energies. This means that band-edge states can visit the surface region as long as they remain orthogonal to the bonded states at the passivation atoms. This condition forces a node of the wave function (which implies that it must be small at the surface), but the first-order correction to the band-edge energies is different from zero, and increases in magnitude as  $E_p$  becomes more electronegative.

#### IV. PASSIVATION-INDUCED CHANGE OF THE CONDUCTION BAND FROM $L$ TO $X$

Figure 1(c) shows the CBM corresponding to electropositive passivants ( $\eta = +5$ ) with  $E_p = E_V + 0.8$  eV, whereas Figs. 1(d) shows the CBM of a highly electronegative passivant ( $\eta = -1$ ) with  $E_p = E_V - 12.9$  eV. We see that for both passivants, that the CBM has a  $\gamma_{6c}$  symmetry, derived from the  $a_1$  orbital<sup>21</sup> symmetry [denoted  $\gamma_{6c}(a_1)$ ]. The Bloch-function content of the CBM changes from  $X_{1c}$ -like for electropositive to  $L_{1c}$ -like for electronegative [see Figs. 1(e) and 1(f)].

The conduction band crossing from  $L$  to  $X$  derived states as  $E_p \rightarrow -\infty$  shown in Figs. 1(e) and 1(f) can be also understood in terms of Eq. (4):  $L$ -derived states are more extended than  $X$ -derived states because of the large effective mass ( $1.57m_e$ ) of the  $L$  minima along the (111) directions. As a consequence,  $L$ -derived states interact more with the passivation potential at the surface. Therefore, a sufficiently deep passivation potential can drag down the  $L$ -derived states.

In a recent paper, Niquet *et al.*,<sup>20</sup> reported calculations of Ge quantum dots with an empirical tight-binding method. Though their method is significantly different from ours, the agreement of their single-particle energies and our calculations<sup>10</sup> is very good. Both calculations show that the optical properties of Ge crystallites remain typical of an indirect-gap semiconductor. As Figs. 1(e) and 1(f) show, the CBM remains indirect (either  $X$ - or  $L$ -like). Both Niquet *et al.*'s,<sup>20</sup> calculations and ours show, however, that there is a significant increase on the reciprocal-space overlap of the CBM and VBM for  $R \approx 15$  Å. However, in contradiction with Niquet *et al.*,<sup>20</sup> we find<sup>10</sup> that such an increase also occurs in spherical dots and not only in cubic ones. However, shape and size can change the symmetry of the band edges, which can make the transition forbidden.

#### V. VALENCE- AND CONDUCTION-BAND CONFINEMENT ENERGIES

One of the interesting quantities measured for quantum dots<sup>9</sup> is the valence-band shift  $\Delta E_{VBM}(R) = -E_{VBM}(R) + E_{VBM}(\infty)$  and the conduction-band shift  $\Delta E_{CBM}(R) = E_{CBM}(R) - E_{CBM}(\infty)$ , where  $E(\infty)$  denotes the energies of the *bulk* band edges. In H-passivated Si dots it was found experimentally<sup>9</sup> that the ratio  $\Delta E_{VBM}(R)/\Delta E_{CBM}(R) \approx 2$ . However, in that experiment  $\Delta E_{CBM}(R)$  included a Coulomb interaction between the electron and the hole:<sup>9</sup>  $J_{Coul}$ . Empirical pseudopotential calculations<sup>11</sup> gave  $\Delta E_{VBM}(R)/(\Delta E_{CBM}(R) - J_{Coul}) \approx 2$ , with a passivation potential that fit the density of states of hydrogenated (001) Si surfaces. Figure 2 gives the values of  $\Delta E_{VBM}(R)/\Delta E_{CBM}(R)$  and  $\Delta E_{VBM}(R)/(\Delta E_{CBM}(R) - J_{Coul})$  for Ge dots as functions of the binding energy of the passivation potential  $E_p$ . We see that for highly electronegative passivants the ratios are 1.3 and 1.8, respectively, but they decrease as the potential becomes shallower. For a wide range of passivations the  $\Delta E_{VBM}(R)/[\Delta E_{CBM}(R) - J_{Coul}]$  ratio is around  $1.5 \pm 0.3$ , which is smaller than the H-passivated Si dot case. Previously, it was generally be-

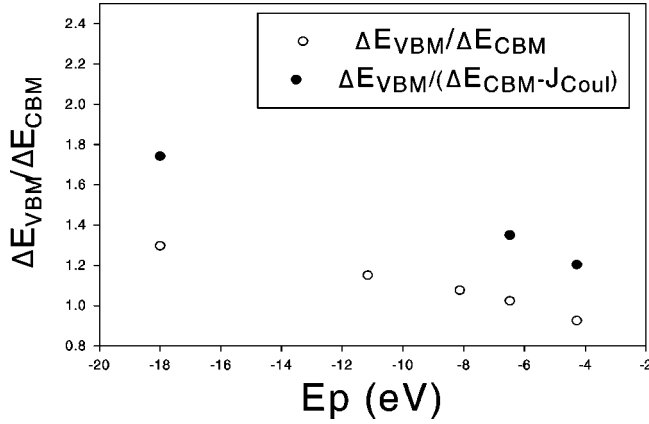


FIG. 2. The ratio of valence-band to conduction-band shift ratio for a 37.4 Å-diameter Ge quantum dot for different surface passivations potentials  $E_p$ .

lied that both conduction- and valence-band shifts are due only to quantum confinement. However, though the amplitude of the wave-function square is four orders of magnitude smaller at the surface passivation atom than at the center of the dot, the integrated effect of all surface atoms can produce a measurable affect. For example, when  $E_p - E_V$  changes from  $-6$  eV to  $+0.8$ ,  $\Delta E_{VBM}(R)$  and  $\Delta E_{CBM}(R)$  change by 11% and 14%, respectively. The gap  $E_g = \Delta E_{VBM}(R) + \Delta E_{CBM}(R) + E_g$  remains almost constant (within 3%) because both the conduction and valence bands are dragged down by the passivation. However, the  $\Delta E_{VBM}(R)/\Delta E_{CBM}(R)$  ratio changes by as much as 30% due to surface passivation.

## VI. OPTICAL CONSEQUENCES

We next discuss the implications of the change from a  $\gamma_{8v}(t_2)$  VBM to a  $\gamma_{8v}(t_1)$  VBM on the excitonic multiplets when spin-orbit and exchange interactions are taken into account. In Fig. 3(I) we discuss case I of Table I, where the VBM is  $\gamma_{8v}(t_2)$  and the CBM  $\gamma_{6c}(a_1)$ ,<sup>21</sup> which is seen<sup>1,2</sup> in conventional direct-gap dots such as InP. In the absence of spin orbit ( $\Delta_{so} = 0$ ) and electron-hole exchange interactions ( $\Delta_x = 0$ ) the  $t_2 \times a_1$  product gives a 12-fold degenerate exciton with  $T_2$  orbital symmetry (column A in Fig. 3 I). Allowance for exchange interaction splits the 12-fold  $T_2$  into a higher-energy spin singlet ( $\times 3$ ) and a lower-energy spin triplet ( $\times 9$ ). The spin and orbital parts of the exciton wave function are mixed by the spin-orbit interaction. But under a weak spin-orbit scenario, the singlets and triplets are almost unmixed. The singlet gives a  $T_2^s$  ( $\times 3$ ), while the triplet splits into  $A_2 + E + T_1 + T_2^t$  (we use Blackboard capital letters to denote symmetry of the full excitonic wave function that mixes spin and orbital components). A scenario with finite spin-orbit and zero exchange  $\Delta_x = 0$  is given in column B of Fig. 3. As the spin-orbit interaction becomes strong, the valence-band maximum  $t_2$  splits into  $\gamma_{8v}(t_2)$  ( $\times 4$ ) and  $\gamma_{7v}(t_2)$  ( $\times 2$ ), separated by the spin-orbit splitting  $\Delta_{so}$ , while the  $a_1$  conduction band maximum gives  $\gamma_{6c}(a_1)$  ( $\times 2$ ). We thus have two families of excitons: those derived from  $\gamma_{8v}(t_2) \times \gamma_{6c}(a_1) = E + T_1 + T_2$ , and those derived from the ‘‘split-off’’ band  $\gamma_{7v}(t_2) \times \gamma_{6c}(a_1) = A_2 + T_2$ . The combined effect of exchange and spin orbit is given in Fig. 3, column C. The exchange interaction affects only the  $T_2$ -symmetric excitons, displacing them to higher energy (shown column A), leaving the forbidden  $E + T_1$  excitons as the ground-state excitons of the  $\gamma_{8v}(t_2) \times \gamma_{6c}(a_1)$  manifold.

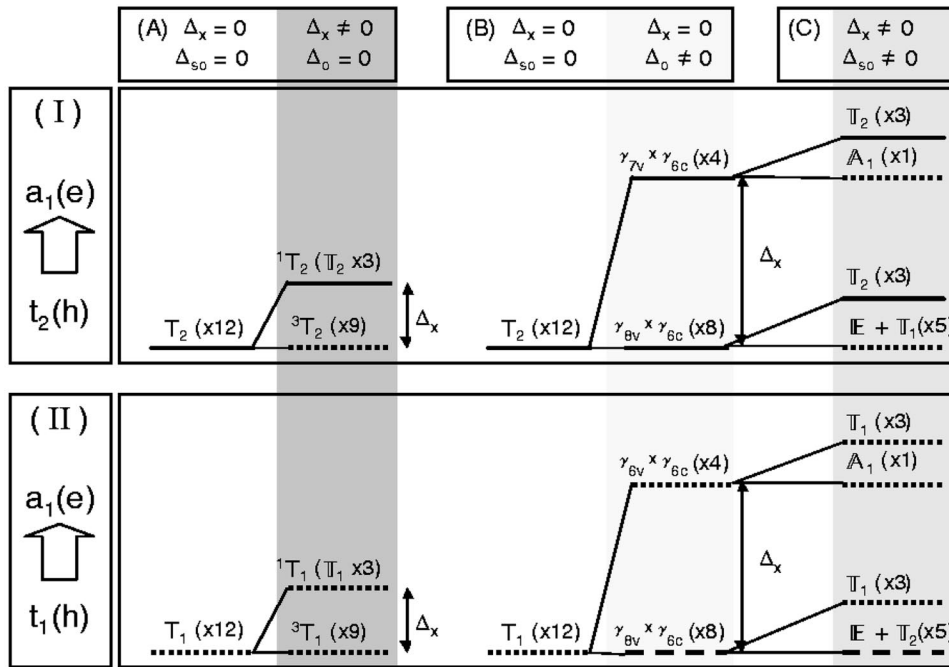


FIG. 3. Structure of the lowest-energy excitonic multiplet as a function of the symmetry of the VBM. (I) corresponds to an electropositive passivation, and (II) to and electronegative passivation.

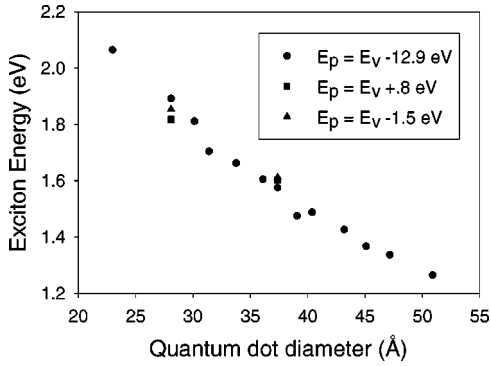


FIG. 4. Excitonic splittings of Ge dots as functions of the quantum dot diameter.

Figure 3(II) shows the case of a  $\gamma_{8v}(t_1)$  VBM, appropriate to dots with electronegative passivation ( $E_p \leq E_v - 1.5$  eV). In the absence of spin-orbit and exchange interactions, the  $t_1 \times a_1$  product gives a 12-fold degenerate exciton with  $T_1$  orbital symmetry. Exchange interaction (column A) split the 12-fold  $T_1$  into a higher-energy spin singlet ( $\times 3$ ) and a lower-energy spin triplet ( $\times 9$ ). The weak spin orbit from the singlet produces an exciton with  $T_1^s$  symmetry, while the triplet states are split into  $A_1 + E + T_1^t + T_2$ . We see that, unlike the previous case, now the exciton multiplet that rises because of exchange has  $T_1$  symmetry (and not  $T_2$ ). In a strong spin-orbit and zero-exchange scenario, (column B in Fig. 3(II)) the  $\gamma_{8v}(t_1) \times \gamma_{6c}(a_1)$  lower-energy family gives  $E + T_1 + T_2$ . The addition of exchange (column C) rises only the states with  $T_1$  symmetry, leaving  $E + T_2$  in the ground state (within the  $t_1 \times a_1$  subspace, the exchange interaction only shifts  $T_1$  symmetric states, as in column A shows). We see that now the ground state has a dipole-allowed component  $T_2$  for the  $\gamma_{8v}(t_1) \times \gamma_{6c}(a_1)$  manifold.

We have next conducted a configuration-interaction calculation<sup>17</sup> for our Ge dots with various passivations. For the electropositive passivation (the first column of Fig. 1), after including spin orbit, exchange interaction, and multiple-configuration couplings<sup>17</sup>, we find the results expected from Fig. 3(I), column C. For this large Ge dot the splitting of the  $T_2$  bright states and the dark ground states is only 1.9 meV. The present calculations for Ge dots include a spin orbit which reduces<sup>1</sup> the exchange splitting by a factor 2/3, as compared with a Si dot of similar size, where the spin-orbit interaction was not included.<sup>8</sup> For this Ge dot size, in the electropositive passivation case [when the VBM is  $\gamma_{8v}(t_2)$ ] the lifetime of the  $T_2$  exciton is one order of magnitude shorter than a similar case corresponding to Si. This is consistent with the fact that Ge dots mix into much more  $\Gamma$  character than Si dots.<sup>10</sup>

For electronegative passivation (second column of Fig. 1) with a  $\gamma_{8v}(t_1)$ -symmetric VBM and a  $\gamma_{6c}(a_1)$ -symmetric CBM, our calculation gives a fivefold ground state with three

partially allowed excitons, as expected from Fig. 3(II), column C. The next states (only 1 meV higher in energy) are a threefold dark multiplet corresponding to the  $T_1$  symmetry. Under electronegative passivation [when the VBM is  $\gamma_{8v}(t_1)$  symmetric], the lifetime of this partially bright  $T_2$  ground level is almost three orders of magnitude longer than the one corresponding to the bright  $T_2$  under electropositive passivation [when the VBM is  $\gamma_{8v}(t_2)$  symmetric]. This results from the fact that for this  $\gamma_{8v}(t_1) \times \gamma_{6c}(a_1)$  exciton manifold the *orbital* symmetry is 99 %  $T_1 + E$ , which gives a zero contribution to the oscillator strength.

The increase in the lifetime of the bright excitons when the passivation is electronegative is a direct consequence of the presence of a node in the envelope function of the VBM. Departures from  $T_d$  symmetry will change the symmetry of the VBM, but the crossing of a nodeless envelope to an envelope with a node will remain. Therefore, we believe that such an increase in the radiative lifetime of the ground-state exciton as a function of passivation will persist if the shape of the dot is close to a sphere.

## VII. EXCITONIC BAND GAP

In Fig. 4 we show our calculated excitonic gap vs size for the lowest-energy exciton for the passivation potential  $E_p = E_v - 12.9$  eV. For comparison we give the results obtained with different passivations ( $E_p = E_v + 0.8$  eV and  $E_p = E_v - 1.5$  eV) for the sizes  $D = 28$  and  $37.2$  Å. On this scale the difference between dark and bright states cannot be resolved. As can be seen, the changes in the excitonic energy induced by the passivation are only significant for the very small size regime, in particular for  $E_p = E_v + 0.8$  eV, as the CBM energy draws close to the passivation potential binding energy and the mixing becomes stronger.

In summary, we have found that surface passivation can drastically modify the lifetime of the lowest-energy states of a Ge quantum dot by introducing a node into the envelope part of the wave function of the VBM. This node in the wave function of the VBM will also appear in nonspherical dots, but strong selection rules will be present only in near spherical dots. Surface passivation can also alter the valence- to conduction-band-shift ratio, without significant changes in the optical gap. We anticipate similar effects in dots made of other materials.

## ACKNOWLEDGMENTS

The authors would like to thank Lin-Wang Wang, A. Williamson, A. Franceschetti, and H. Fu for supplying some of the programs used in this work, and for stimulating discussions, and M. L. Bruschi and R. Trincherro for discussions on the treatment of the double symmetry group. This work was supported by OER-BES-DMS under Contract No. DE-AC36-99-GO10337.

\*Present address: Centro Atómico Bariloche, (8400) S. C. de Bariloche, Río Negro, Argentina.

<sup>1</sup>M. Chamarro, M. Dib, V. Voliotis, A. Filoramo, P. Roussignol,

T. Gacoin, J. P. Boilot, C. Delerue, G. Allan, and M. Lannoo, Phys. Rev. B **57**, 3729 (1998).

<sup>2</sup>K. Leung and K. B. Whaley, Phys. Rev. B **56**, 7455 (1997); K.

- Leung, S. Pokrant, and K. B. Whaley, *ibid.* **57**, 12 291 (1998).
- <sup>3</sup>G. B. Grigoryan, E. M. Kazaryan, Al. L. Efros, and T. V. Yazeva, *Zh. Éksp. Teor. Fiz.* **32**, 1772 (1990) [*Sov. Phys. Solid State* **32**, 1031 (1990)].
- <sup>4</sup>Al. L. Efros and A. V. Rodina, *Solid State Commun.* **72**, 645 (1984).
- <sup>5</sup>The spin orbit is negligible compared to the quantum confinement energy of the VBM.
- <sup>6</sup>B. Delley and E. F. Steigmeier, *Phys. Rev. B* **47**, 1397 (1993).
- <sup>7</sup>S. Y. Ren, *Phys. Rev. B* **55**, 4665 (1997); *Solid State Commun.* **102**, 479 (1997).
- <sup>8</sup>F. A. Reboredo, A. Franceschetti, and A. Zunger, *Phys. Rev. B* **61**, 13 073 (2000).
- <sup>9</sup>T. van Buuren, L. N. Dinh, L. L. Chase, W. J. Siekhaus, and L. J. Terminello, *Phys. Rev. Lett.* **80**, 3803 (1998).
- <sup>10</sup>F. A. Reboredo and A. Zunger, *Phys. Rev. B* **62**, R2275 (2000).
- <sup>11</sup>L. W. Wang and A. Zunger, in *Semiconductor Nanostructures*, edited by P. V. Kamat and D. Meisel (Elsevier, New York, 1996), (Vol. 103).
- <sup>12</sup>L. W. Wang and A. Zunger, *Phys. Rev. B* **51**, 13 798 (1995).
- <sup>13</sup>Because of the energy cutoff in the kinetic energy of the plane-wave expansion, the real-space potential felt by the electrons is not a closed formula. Accordingly, it is better to characterize the passivation potentials with respect to its bond state.
- <sup>14</sup>The binding energies of  $v_p^\eta(q)$  are calculated by placing an isolated passivating atom in the supercell.
- <sup>15</sup>G. F. Koster, in *Solid State Physics*, edited by F. Seitz and D. Turnbull (Academic Press, New York, 1957), Vol. 5, p. 173.
- <sup>16</sup>C. Cohen-Tannoudji, B. Diu, and F. Laloë, in *Quantum Mechanics* (Wiley, New York, 1977), Vol. II, p. 984.
- <sup>17</sup>A. Franceschetti, H. Fu, L. W. Wang, and A. Zunger, *Phys. Rev. B* **60**, 1819 (1999).
- <sup>18</sup>The spin-orbit coupling splits  $t_2$  states into  $t_2 \times \gamma_6 = \gamma_{8v}(t_2) + \gamma_{6v}(t_2)$ ,  $t_1$  states into  $t_1 \times \gamma_6 = \gamma_{8v}(t_1) + \gamma_7(t_1)$ , and  $e$  states into  $e \times \gamma_6 = \gamma_{8v}(e)$ . Because  $\gamma_{8v}(t_2)$ ,  $\gamma_{8v}(t_1)$ , and  $\gamma_{8v}(e)$  have the same symmetry, they can be mixed by the spin-orbit interaction.
- <sup>19</sup>J. B. Xia and K. W. Cheah, *Phys. Rev. B* **59**, 14 876 (1999).
- <sup>20</sup>Y. M. Niquet, G. Allan, C. Delerue, and M. Lannoo, *Appl. Phys. Lett.* **77**, 1182 (2000).
- <sup>21</sup>The  $\gamma_{6c}(a_1)$  symmetry is very frequent in the  $L$ -to- $X$  crossover region where the  $L$ - $X$  mixing lowers the energy of the  $\gamma_{6c}(a_1)$  CBM states.